Cedar Creek Reservoir
Sediment Density and Channel Erosion Study

Overview

1. Map of the reservoir shoreline and core sample locations.
2. Written report describing the methods and results of the cores and densities and the relationship to acoustic data taken at each core site
3. Map of potential sources of sediment within the watershed other than sheet and rill erosion; namely gully and channel erosion.
4. General estimates of potential volumes of erosion from channel sources within the watershed based on assumptions of degradation, widening.

These items are compiled within three separate sections:

Section I: Details the coring operations, estimates of the sediment density, and total estimated volume of sediment in the reservoir.
Section II: Describes field assessment of channel and gully erosion and assesses potential channel erosion volumes using numerous methodologies.
Section III: Describes temporal changes in erosion as observed on air photographs taken from about 1940 to 2000.

Summary

(1) The coring results from this study, which were taken from only five points spread over the reservoir, indicated an average sediment thickness of **1.29 ft.** versus 1.6 ft. from the TWDB reports. Assuming an average dry-weight density for the sediment of **21.5 lbs/ft^3**, from this study, the annual sedimentation rate in the reservoir is estimated to be **492,247** tons.

(2) The mean channel erosion rate in the watershed is estimated to be **165,504** tons or up to 34 percent of the total sediment

delivery to the reservoir based on 6 methods. Channel erosion could increase by a factor of 3 if channels begin to degrade.

(3) No major land uses changes have occurred over the whole basin. There is a general shift from agriculture to pasture which is similar to a lot of areas on the urban fringe in Texas. The major growth area appears to be in the northwest portion of the watershed which is urbanizing. The air photos indicate major changes in processes in the sand terrain are related to major climate cycles; processes in the clay terrain appear less influenced by broad scale climatic changes but are influenced by urban land use changes. Clay channels are very susceptible to changes in channel slope due to channelization or increases in discharge which can result in rapid channel degradation and widening.

Sincerely,

SDI, Inc and Peter M. Allen, John Dunbar, Shane Prochnow and Lisa Zygo, April 2006.

Acknowledgements: John Bongino for field assistance, and Jeff Arnold for communication on the SWAT model output.

Section I: Coring Operations

Vibracore method. To determine the thickness and dry weight of post-impoundment sediment in Cedar Creek Reservoir, we collected sediment cores at five locations distributed over the length of the reservoir (Figure 1). Vibracoring is standard method for obtaining undisturbed cores of unconsolidated sediment at saturated or nearly saturated conditions (Lanesky et al., 1979; Smith, 1984). The vibracore device uses a 1-HP motor that drives a pair of weights that are eccentrically mounted on two counter rotating shafts. The motor and vibrator mechanism is housed within a watertight aluminum chamber so it can be immersed in water. The vibracore motor is powered by two 12-volt batteries connected in series through a 150-ft power cord, thus limiting the depth of operation. A 35 lb ring-weight is added to the vibrator to provide downward force for penetration. The chamber is connected to the top of a 76 cm (3 in.) diameter aluminum core tube. Core-catcher devices, consisting of interlocking aluminum fingers, are riveted to the inside of the bottom of the core tubes. The core-catchers flatten to the inside of the tube during penetration, allowing the core sample to slide into the tube without being disturbed. Then during retrieval, the fingers lock to prevent the core sample from sliding back out of the tube. The vibrator, ring weight, and full core tube weigh approximately 100 lbs. To pull a long core tube out of the bottom requires 200-300 lbs of additional lift capacity. For this reason the vibrator system is deployed using a tripod gantry with hand-winch mounted on the front of the survey boat (Figure 2).

Cores are collected by lowering the vibrator with core tube attached to the bottom by the hand winch, turning on the vibrator, and allowing the tube to slowing vibrate into the bottom. The vibration causes the sediment to liquefy in a region a few millimeters thick near the tube wall, allowing the tube to slide into the sediment with little drag. This results in less disturbance and compaction of the sediment cores than occurs with gravity-driven drop coring devices. Lengths of core tube 4 to 12 ft (1.2 to 3.7 m) long can be easily driven into soft sediment. Penetration of stiff pre-impoundment soils is normally limited to 6 inches (.152 m) or less. When the core tube had reached the point of refusal, the vibrator was turned off and the core was winched out of the bottom. On deck, the retrieved cores were capped top and bottom with rubber end-caps and stored upright during transport.

Core analysis. The goal of our coring operation was to determine the thickness and dry-weight density of the post-impoundment sediment present at representative sites along the axis of the reservoir. To identify the base of post-impoundment sediment in the cores, we relied on visual examination of the sampled material, and measurements of the sediment water content and sediment strength versus depth in the cores. After the cores were brought back from the field, they were sub-sampled by cutting the core tube and sediment into 5-cm slices using a pipe cutter. During the sub-sampling operation the strength of the sediment was determined using a pocket penetrometer that measures the force required to drive a 2.5 cm diameter disk into the sediment. These tests were performed on the top of each 5 cm sample, while the sample was confined in the core tube. The sediment within each 5 cm slice was weighed, dried for 48 hours at 106º C, reweighed, and stored for potential future analysis. The wet and dry weights of the samples were used to compute water content versus depth within the cores. From the average water content fraction of sampled sediment *wc*, we estimate the average dry-weight density ρ_{dw} of the sediment within each core using the formula

$$\rho_{dw} = \frac{\rho_w \rho_g (1 - wc)}{\rho_g (wc) + \rho_w (1 - wc)}, \tag{1}$$

where ρ_w is the assumed density of water (1000 kg/m^3) and ρ_g is the assumed density of the sediment grains (2600 kg/m^3).

Coring field procedures. Cedar Creek Reservoir is a relatively long (30 km) and narrow (3 km) lake. The position of each core site along the long axis of the reservoir was pre-selected to provide representative cores for each part of the reservoir (backwater, mid-lake, and main basin). At the general pre-selected positions for core sites 1, 2, and 3, the placement of the actual core sites across the short axis of the lake were selected with the aid of acoustic sub-bottom profiling. We initially profiled across the lake, while monitoring the sediment thickness in real time on the profiler display. Then we collected a core at a site where the sediment thickness appeared to be representative of the thickness along the cross-section. Between core sites 1, 2, and 3 we monitored sediment thickness continuously along axial profiles to check for potential variation in sediment thickness along the axis of the reservoir. <u>No significant sediment thickness variations were observed</u>. The sediment thickness appeared to vary between 1 and 2 ft throughout. Boat speed while profiling is limited to 5 miles and hour. Hence, to collect cores 4 and 5, we pulled the profiler unit and ran the length of the lake at 15 mph and sited these last two cores in the backwater region without the aid of acoustic profiling. The geographic position of each core site was determined using differential corrected GPS positioning, while anchored at the sites.

Coring results. All five cores collected in Cedar Creek Reservoir penetrated 30 to 45 cm (1 to 1.5 ft) of high water content (62 to 76%), organic-rich mud and then into the upper 5 cm of a highly compacted, black clay, with soil texture (peds) and traces of plant roots. The high water content mud is interpreted to be post-impoundment sediment and the compacted soil is interpreted to be the pre-impoundment surface. The corresponding average dry-weight density for the post-impoundment sediment, computed with equation 1, is 344.5 kg/m^3 (<u>21.5 lbs/ft^3</u>). Results for the individual cores are given in Figure 3 and Tables 1-5.

Sediment dry weight. From prior coring results for other reservoirs within the Blackland Prairie (Aquilla, Granger, Limestone, and 12 SCS flood control reservoirs), post-impoundment sediment in Blackland reservoirs commonly have an average water content that ranges from 60 to 68%, which corresponds to an average dry-weight density of 400 to 560 kg/m^3 (25 to 35 lbs/ft^3). With the exception of Core 5, from the backwater region of the reservoir, the cores from Cedar Creek Reservoir have higher water content and lower dry-weight density than typical for the Blackland Prairie. As a result, the dry weight of sediment in the reservoir is likely less than would normally be associated with the same volume of sediment in other Blackland reservoirs.

The latest volumetric survey of Cedar Creek Reservoir was conducted by the Texas Water Development Board (TWDB) in March, 2005 (TWDB, 2006). This survey indicated that the reservoir had a remaining water storage volume at the normal pool elevation of 637,924 acre-ft in 2005, compared to an initial volume of 679,200 acre-ft in 1965. This corresponds to a volume loss of 41,276 acre-ft in the 40 year period between 1965 and 2005. The volume loss is attributed to the deposition of sediment from the supplying watershed. Multiplying this sediment volume the average dry weight density determined in the current study indicates that the total dry weight of the sediment is 19,296,060 tons. The corresponding average annual sediment deposition rate from 1965 to 2005 is 482,400 tons/yr. Assuming a sediment trap efficiency for the reservoir of 98%, the expected average sediment yield from the supplying watershed is <u>492,247 tons/yr.</u>

Discussion of coring results. The estimated sediment yield of 492,247 tons/yr is based on the coring operations described in this report and on the TWDB 2005 survey, which accounted for the first 40 years of sedimentation (1965 to 2005). One approach to checking the validity of the TWDB survey is to compare the average sediment thickness predicted by the survey to the average thickness indicated by the coring results. To do this we first scale the estimated volume change to account for one additional year of sediment accumulation between the March, 2005 survey and the late February, 2006 coring operation to produce an estimated 2006 sediment volume of 42,308 acre-ft. We then divided this volume by the surface area of the reservoir reported in the 2005 survey (32,873 acres) to compute an average sediment thickness of 1.29 ft (39.2 cm). This average thickness differs from the average thickness determined by coring (37.4 cm) by less than 5%, and is within the range of thicknesses observed in the cores (30 to 45 cm). Given the sparse core sampling and the one-year extrapolation of the TWDB results, these estimated sediment thicknesses are in reasonable agreement. Assuming the lower average sediment thickness from this study, the corresponding annual sediment yield from the watershed is 481,082 tons/yr. The range from 481,082 to 492,247 tons/yr reflects the level of uncertainty in the average annual sediment yield over the last 40 years.

The methods used in this study to estimate long term sediment yield were chosen as a compromise between accuracy and economics. The most accurate estimates of long term sediment yield would be produced by conducting a modern sediment survey, combining sub-bottom acoustic profiling, to measure and map sediment thickness throughout the reservoir, with a coring program, like the one done in this study. The cores provide much better estimates of sediment density. Assuming regional averages for sediment density can easily produce errors of 50 to 80% in the estimate of the dry sediment weight. The advantage of the sub-bottom profiling method is that sediment thickness is measured directly, rather than being inferred by the apparent change in overall volume. Sediment volumes estimated from the change in water volumes are influenced by accumulated error in the initial and final surveys. In the case of Cedar Creek Reservoir, it lost only 6% of its original volume in 40 years. If both the initial and final surveys were in error by 2 to 3 %, the resulting sediment volume estimate could be in error by 75 to 100%.

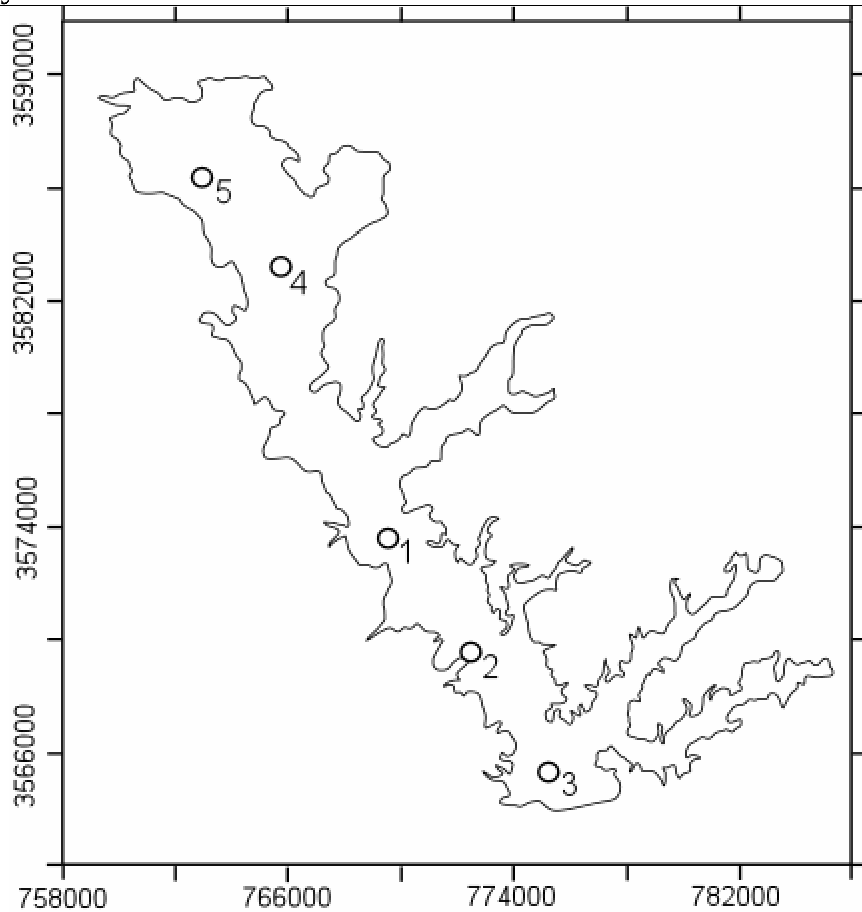

Figure 1. Coring locations in Cedar Creek Reservoir. Geographic coordinates are UTM Zone 14, meters.

a. b.

Figure 2. Coring operations on Cedar Creek Reservoir. (a) Coring gantry on from of survey boat. (b) Retrieving a core.

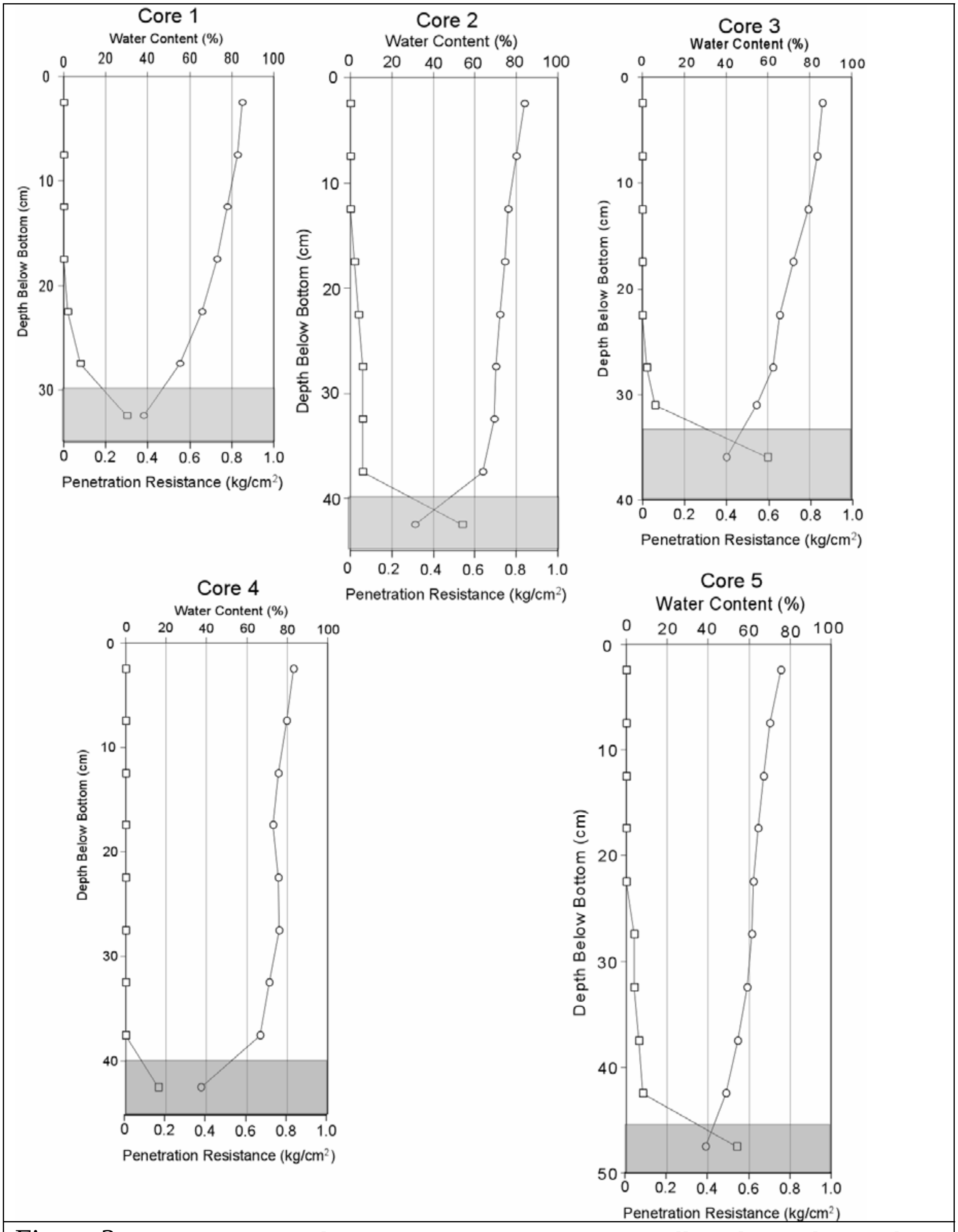

Figure 3. Water content and penetration resistance in cores collected in Cedar Creek Reservoir. Circles mark the variation in water content by weight. Squares mark the variation in penetration resistance. The regions of the graphs with white background correspond to the post-impoundment sediment. The regions with gray background correspond to the underlying pre-impoundment soil.

Table 1. Core 1 sub-sampling results. Top is depth below the water bottom to the top of the sub-sample (cm), Bottom is the depth below the water bottom to the bottom of the sub-sample (cm), Cont wt is the sample container weight (g), Wet is the weight of the wet sample in the container (g), Dry is the dry weight of the sample in the container (g), Water cont is the water content by weight (%), and Pen is the sample penetration resistance in kg/cm^2. Table entrees with white background correspond to post-impoundment sediment. Table entrees with gray background correspond to pre-impoundment soil.

Sample	**Top**	**Bottom**	**Cont wt**	**Wet**	**Dry**	**Water cont**	**Pen**
1	0	5.0	8.56	188.45	35.5	85.024181	0
2	5	10.0	8.4	192.06	40.07	82.75618	0
3	10	15.0	8.22	289.11	70.02	77.998505	0
4	15	20.0	8.61	283.81	83.25	72.877907	0
5	20	25.0	8.33	303.16	109.49	65.688702	0.02
6	25	30.0	8.15	171.3	81.03	55.329451	0.08
7	30	35.0	8.4	297.15	187.04	38.133333	0.3

Table 2. Core 2 sub-sampling results.

Sample	**Top**	**Bottom**	**Cont wt**	**Wet**	**Dry**	**Water cont**	**Pen**
1	0	5.0	8.47	196.3	38.88	83.809828	0
2	5	10.0	8.34	219.04	50.51	79.985762	0
3	10	15.0	8.39	247.15	65.66	76.01357	0
4	15	20.0	8.47	276.24	76.6	74.556522	0.02
5	20	25.0	8.19	261.3	78.55	72.201809	0.04
6	25	30.0	8.1	219.4	71.02	70.222433	0.06
7	30	35.0	8.44	286.86	94.12	69.226349	0.06
8	35	40.0	8.38	230.67	89.31	63.592604	0.06
9	40	45.0	8.45	293.66	204.87	31.131447	0.54

Table 3. Core 3 sub-sampling results.

Sample	**Top**	**Bottom**	**Cont wt**	**Wet**	**Dry**	**Water cont**	**Pen**
1	0	5.0	8.37	180.19	32.48	85.967873	0
2	5	10.0	8.29	215.67	42.36	83.571222	0
3	10	15.0	8.5	246.32	58.19	79.106047	0
4	15	20.0	8.31	261.78	79.34	71.97696	0
5	20	25.0	8.32	258.42	94.18	65.669732	0
6	25	30.0	8.43	235.52	94.15	62.252851	0.02
7	30	32.0	8.25	126.47	62.1	54.449332	0.06
8	32	40.0	8.33	309.75	188.49	40.22958	0.6

Table 4. Core 4 sub-sampling results.

Sample	Top	Bottom	Cont wt	Wet	Dry	Water cont	Pen
1	0	5.0	8.6	144.81	31.82	82.95279	0
2	5	10.0	8.57	197.08	46.88	79.67747	0
3	10	15.0	8.55	221.88	61.03	75.39962	0
4	15	20.0	8.47	233.62	69.35	72.96025	0
5	20	25.0	8.55	277	74.07	75.59322	0
6	25	30.0	8.49	251.8	67.25	75.84974	0
7	30	35.0	8.3	263.81	82.1	71.11659	0
8	35	40.0	8.39	263.1	93.19	66.70724	0
9	40	45.0	8.41	349.58	222.84	37.14864	0.16

Table 5. Core 5 sub-sampling results.

Sample	**Top**	**Bottom**	**Cont wt**	**Wet**	**Dry**	**Water cont**	**Pen**
1	0	5.0	8.53	224.09	61.58	75.389683	0
2	5	10.0	8.55	289.64	92.14	70.262194	0
3	10	15.0	8.36	294.08	102.16	67.170657	0
4	15	20.0	8.74	234.46	89.27	64.323055	0
5	20	25.0	8.39	263.81	105.45	61.999843	0
6	25	30.0	8.29	279.8	113.79	61.143236	0.04
7	30	35.0	8.55	284.82	121.35	59.170377	0.04
8	35	40.0	8.5	322.59	151.69	54.411156	0.06
9	40	45.0	8.51	201.89	107.78	48.665839	0.08
10	45	50.0	8.25	330.47	205.36	38.827509	0.54

Section II: Channel Erosion Estimates

Mean channel erosion in the Cedar Creek Watershed is estimated to be 165,504 tons per year. This is based on six different methods of channel erosion assessment: (1) erosion assessment made for the basin based on NRCS field evidence (Griener, 1982), (2) field assessment of channel erosion and SWAT generated channel lengths and dimensions, (3) field assessment of channel erosion and integrating erosion over the length of the channel, and (4) using power functions utilized in SEDNET (Wilkinson, et. al. 2004), (5) comparison of erosion rates to gage data by Ecoregion after Simon, et. al. (2004) and (6) literature review of channel erosion rates.

Project Area

Creek Reservoir has a drainage area of approximately 2608 sq. km. (1,007 sq. mi.) at USGS Gage Site 0863010. The reservoir began impoundment in July of 1965 and was completed in February 1966. The capacity at conservation pool level is 637,200 acre feet. The watershed trends approximately along strike of four major geologic units. From oldest to youngest these are: Cretaceous Neylandville marl, Cretaceous Nacatoch sand, Tertiary Midway Group and Tertiary Wilcox. For simplicity, a land resources map of the area is shown which simplifies the geologic map into general lithologic (rock types) units, Figure 4 and Table 6.

.

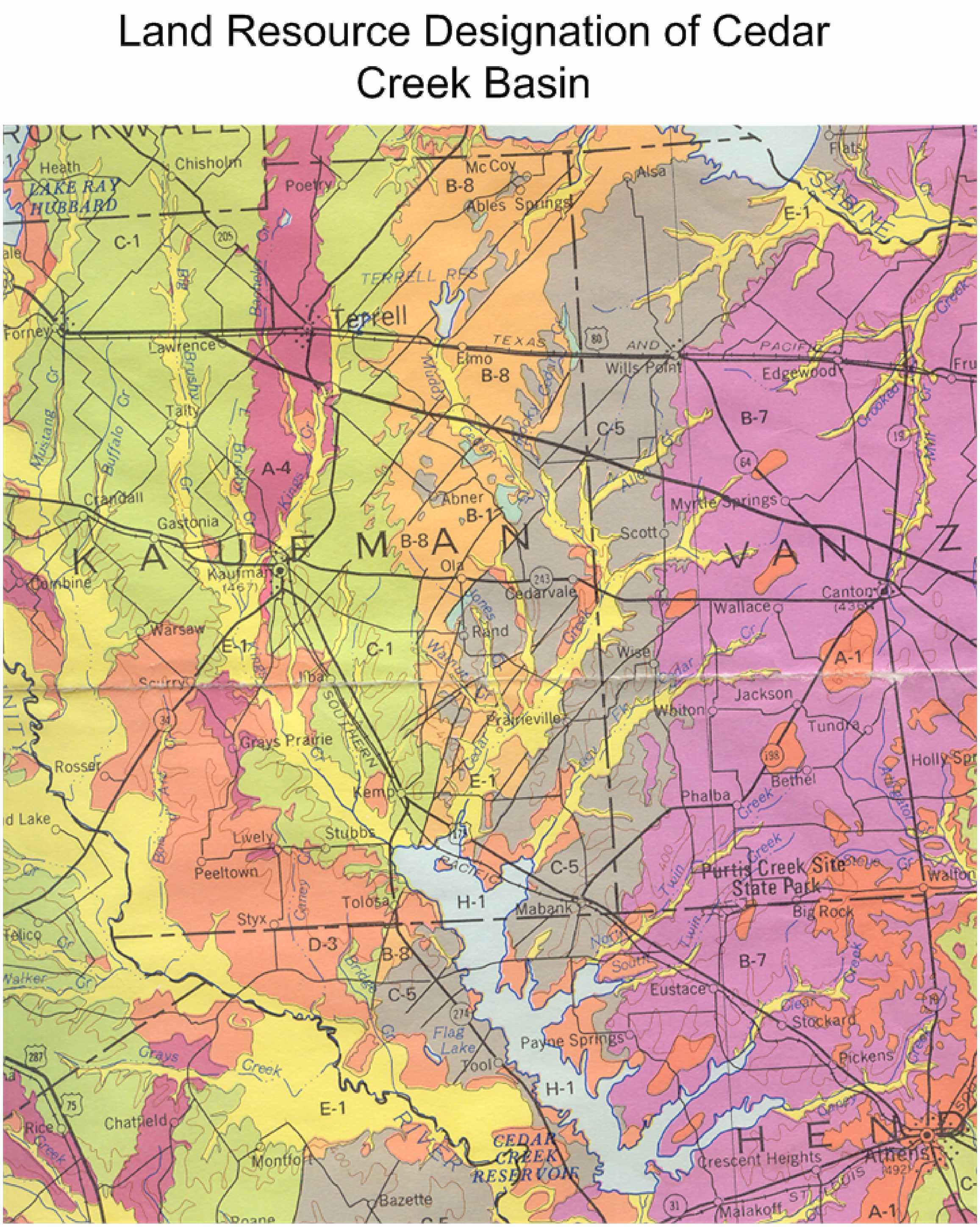

Source: Kier and Others (1977)

Figure 4. Land Resources Map of the Cedar Creek Watershed.

Map Unit	Substrate	Soils	Slope Stability	Plasticity
C-1	Smectitic clay	Dark calcareous clay	Low	High
A-4	Muddy sand and alluvial material	Sandy-clayey loams	Low to high	Low to Moderate
B-8	Glauconitic sand; locally clayey	Thin to moderately thick clayey sand	Moderate to high	low
C-5	Quartz sand and clay, some silt	Clay and sandy loams	Moderate	Moderate to high
B-7	Kaolinitic clay and lignite; local quartz sand	Clay loams	Low to moderate	Moderate

Table 6. Description of Land Resources Units in Basin (After Kier and others, 1977).

In general, it can be seen that the C-1 and B-7 mapping units have more clayey substrates while the other units are sandier. Except for the clays of the C-1 Unit, the majority of the soils are predominantly sandy and clayey loams.

Methods

Greiner Method

Griener (1982) summarized sediment yield for 300 points within the State of Texas based on modeled and field observations by the NRCS. Gross gully and stream bank erosion was obtained from analyzing a national resource inventory in which 4753 primary sample units consisting of 160 acres in size were expanded to the watershed scale to arrive at estimates of annual gross gully and streambank erosion. A gully-stream delivery ratio was then used to compute the total erosion to the yield point from the watershed where:

$$DR = 69.49 \text{ X } 2.7128^{(.0000001644 \text{ X Acres})} \quad (1)$$

Land Area (ac.)	Gross Sheet and Rill (Tons/ac.)	Gross Gully and Streambank (Tons/ac.)	Controlled Drainage (ac.)	Sediment Yeild (Tons/ac.)
612,017	1.26	0.64	365,447	0.33

Table 7. Sediment Erosion Results from Griener, (1982), Table 46, page 83.

In Griener's method, he estimated sediment delivered to "yield points" within the State of Texas (Table 7). Yeild points were major river junctions or reservoirs. In order to do this it was necessary to determine the trapping elements within the drainage area above each yield point. Estimates were made of sediment delivered to and bypassing all trapping elements in the watershed which then followed downstream and contributed to the total sediment load at the yield points. The area behind the trapping elements was termed "controlled drainage". The trapping elements consisted of upstream reservoirs and floodwater retarding structures. In the Cedar Creek Watershed, Griener computed a total of 365,447 acres of controlled drainage (Greiner, 1982, Table 46, page 83).

Assuming a 90% trap efficiency, the yield for the Cedar Creek Basin would be from a the contributing area of 246,570 acres or 385.3 square miles. This is equivalent to a contributing drainage area of 279,558 square miles with no upstream contols. This computes to <u>129,357 tons per year from gully and stream bank erosion</u> (using a the delivery ratio 0.723 adjusted for contributing area). Sheet and rill erosion, accounting for the same contributing area would be 70,449 tons (using a delivery ratio of .2). The total according to these calculations would be about <u>199,806</u> tons per year to the reservoir. About <u>65 percent of the sediment would be from channel and gully erosion; about 35% would be from sheet/rill.</u> These calculations are consistent with Griener's calculation of about 0.33 tons/acre for the watershed (199,806/612,017).

Wilkinson Method

The SWAT model was run for the Cedar Creek Watershed by the Spatial Sciences Lab at Texas A&M. The stream erosion component of the SWAT model utilizes routing reaches which are compiled by subwatershed. Field assessment of streams within the watershed was performed to assess the potential channel erosion rate of a sampling of stream reaches (n=56) within the Cedar Creek Watershed. In general, two types of channel erosion can be observed. In typical streams, channels erode principally on the outside of meanders, Figure 5. Therefore, lateral erosion rates reflect erosion on one side of the channel; volumetric loss is calculated by the product of channel length times the erosion rate and the soil density and eroded channel height equation (2) . The erosion rate is based on observations of the severity of erosion viewed in the field and literature.

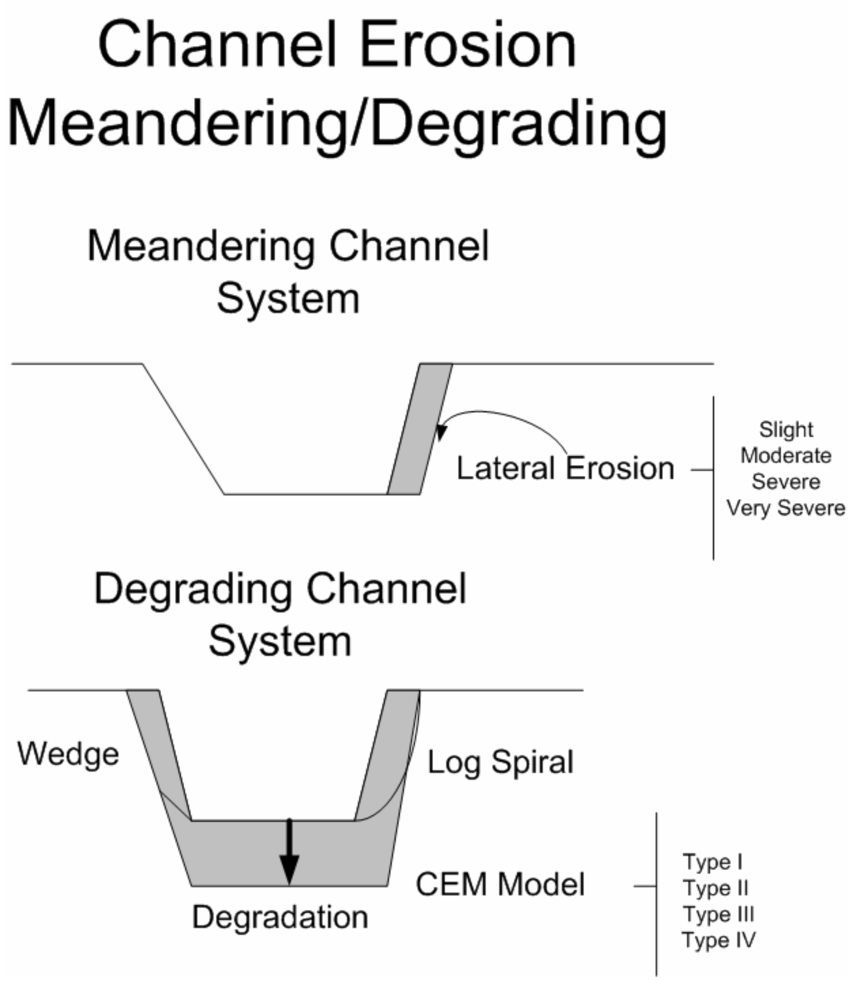

Figure 5. Simplified Channel Erosion Types

Sampling methods were based on previous work by Windhorn (2001) and others. The lateral recession rate estimates were based on visual examination of banks in the field according to Table 8, and shown in Figure 6. Figure 6 was compiled mainly from field evaluation of streams as seen from stops indicated on the map and detailed in the Appendix. While air photographs were used, it was found that the quality of existing photographs, (except for Brushy Creek) were not sufficient quality to use to delineate the erosion characteristics of the smaller streams. Therefore, based on land use, stream condition at surveyed locations, and minor use of sequential air photographs, the maps categories were extended between field locations. This map should be used as a preliminary estimate of existing stream conditions within the reach. Future studies which involve higher resolution photographs or perhaps digital video shots of the channels from helicopters (which have been used in some statewide studies) would improve precision of the map.

Lateral Recession Rate (ft/yr.)	Average (ft./year)	Category	Description
0.01-0.12	.0675	Slight	Some bare bank but active erosion not readily apparent. Some rills but no vegetative overhang. No exposed tree roots.
0.2-0.8	.5	Moderate	Bank is predominantly bare with some rills and vegetative overhang. Some exposed tree roots. No slumps.
0.5-1.4	.94	Severe	Bank is bare with very noticeable vegetative overhang. Many tree roots exposed and some fallen trees. Slumping or rotational failures are present. Some changes in cultural features such as missing fence posts and realignment of roads.

Table 8. Field Evaluation Criteria for Channel Erosion Assessment after Windhorn (2001) and studies in Arkansas, Colorado and Carolina.

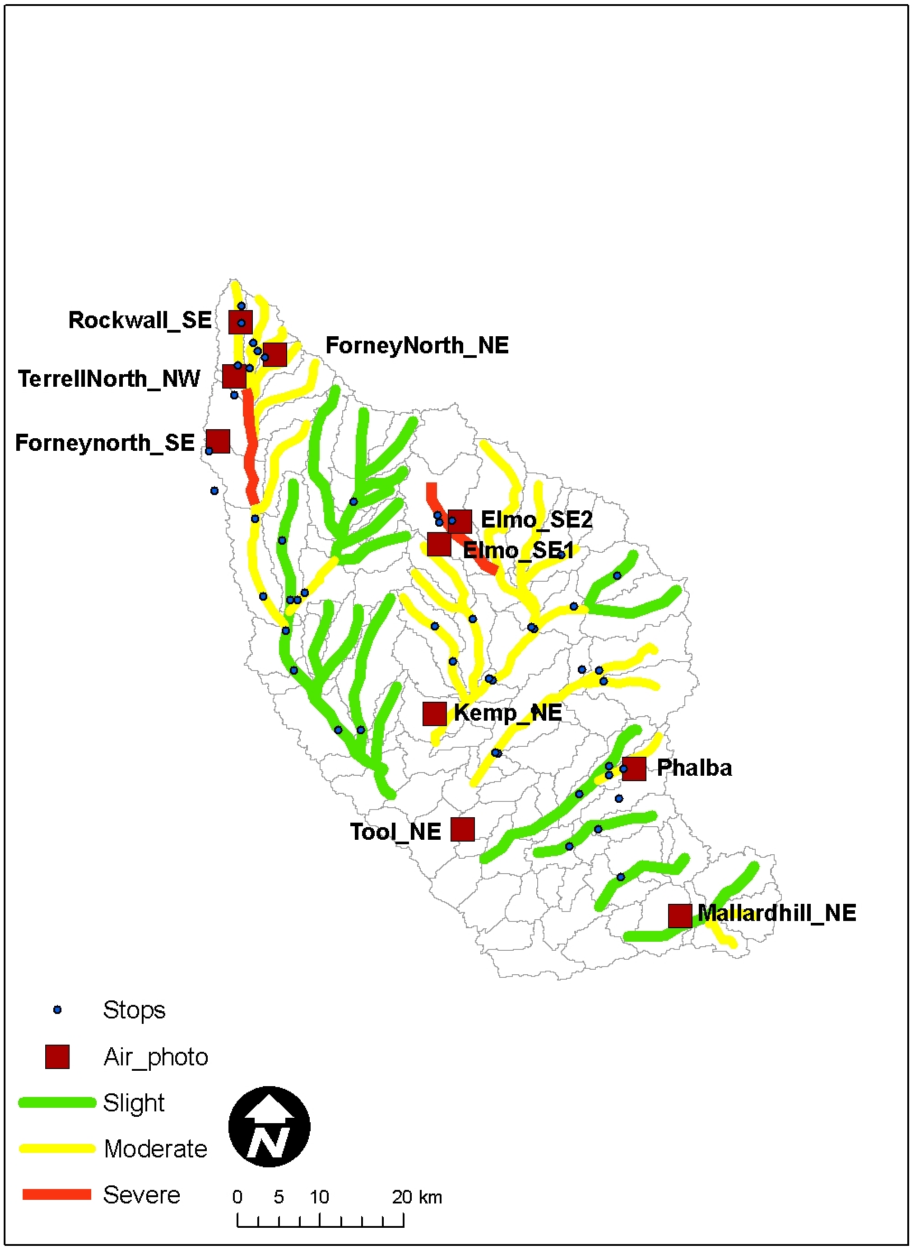

Figure 6. Field Assessment of Channel Erosion and Historic Photograph Sites.

In addition to categorizing the channel for lateral erosion, the Channel Evolution Model (CEM) was used to assess the stage of channel adjustment and potential degree of downcutting. According to Schumm and others (1984), channels follow a predictable pattern of adjustment with time when changes occur in the watershed such as land use, or channelization, or structural (dams, etc.). The pattern of adjustment varies along the longitudinal profile of the channel, depending on the channel slope and sediment supply. This sequence has been elaborated by Simon (1986;1994) who have shown that the sequence can be described as a series of steps toward equilibrium channel conditions. This sequence is often referred to as the Channel Evolution Model (CEM). A simplified figure illustrating the channel Types I-IV which illustrate each step is shown, Figure 4. In general, Type I represents the original channel prior to downcutting. In Type II channels, the major process is degradation, typically through the advance of knickpoints. As the channel downcuts, the sideslopes are oversteepened and the channel banks begin to fail. In Type III channels, the channel is still downcutting, but widening is the major process. As the channel downcuts and widens, it slowly begins to reach a new channel slope which is able to transport the available bed material downstream without long term degradation or aggradation. The channel has now established a new channel and floodplain and begins to establish a new channel and floodplain within this area. At each site, (Appendix 1.). survey forms were used to categorize the level of channel incision as well as degree of erosion Figure 12. Typically, signs of degradation noted in the field include knickpoints, erosion on both banks, entrenchment ratios less than 2.2.

At each location the channel was photographed and average site dimensions were taken with range pole and hand held laser. Accuracies are probably plus or minus 2 feet. Two channel properties were calculated from the measurements; the width depth ratio and the entrenchment ratio. The width depth ratio is here defined as the ratio of the width of the active channel seen in the field to the depth of the active channel. This ratio is important in understanding the energy within the channel and the ability of the discharge frequency to move sediment. The mean width depth ratio was 6.6 (std. dev. 3.2) and the range was from 2-21.The active channel has been shown by Allen, et. al.(2002) to correspond to the bankfull channel in North Texas streams.

The entrenchment ratio in this study is defined as the ratio of the width at the active channel depth to the width at 2X the active channel depth. With a mean side slope of 52 degrees, this computed to a mean value of 1.27 (std. dev. 0.134) and a range of 1.07 to 1.66 for all the sample sites. According to Rosgen (1996), a channel is by definition entrenched when the ratio is below

1.4. From 1.4 to 2.2 a stream is classified as moderately entrenched and above 2.2; slightly entrenched. All channels surveyed were entrenched using the definition and the described method. An entrenched stream will contain larger floods and thus be more prone to frequent channel erosion. While more exacting work which entails more detailed channel measurements should be done on hydraulic geometry relations, the following tend to support the thesis that the channels are entrenched and that channel erosion, can be a major source of sediment in the watershed; especially if land use changes enhance discharge.

Channels were rated based on severity of present erosion and based on the CEM Channel Evolution Model Type. In general, Type II-III channels were more evident in the northwestern portion of the basin in the outcropping area of the Cretaceous Neylandville (C-1) on Big Brushy Creek and then again in the area of the Tertiary aged Midway (B-8) along the Muddy Cedar Creek. The encroachment of urbanization in the upper reaches of Big Brushy Creek is apparently beginning to effect discharge and some channel modifications are visible. In some areas, as locations 2 and 39, it appears as if the channel has gone through one set of downcutting and widening and is currently in Stage IV, (Figure 13). Changes in land use, channel straightening or changes which result in greater discharge can reactivate the system.

Typical channel ratings and sites within the basin are shown in Figures 8 through 11 and given in Appendix. If the channels are moving into stage II-III, erosion should probably be adjusted to reflect sediment loss from both banks and the channel bottom as has been shown by Simon, e.t al. 2004. For this study, all channel erosion was estimated assuming CEM 1 or one channel eroding. It was not felt that resolution of the CEM stages throughout the system was good enough to incorporate the increased erosion into the estimates. (See Conclusions).

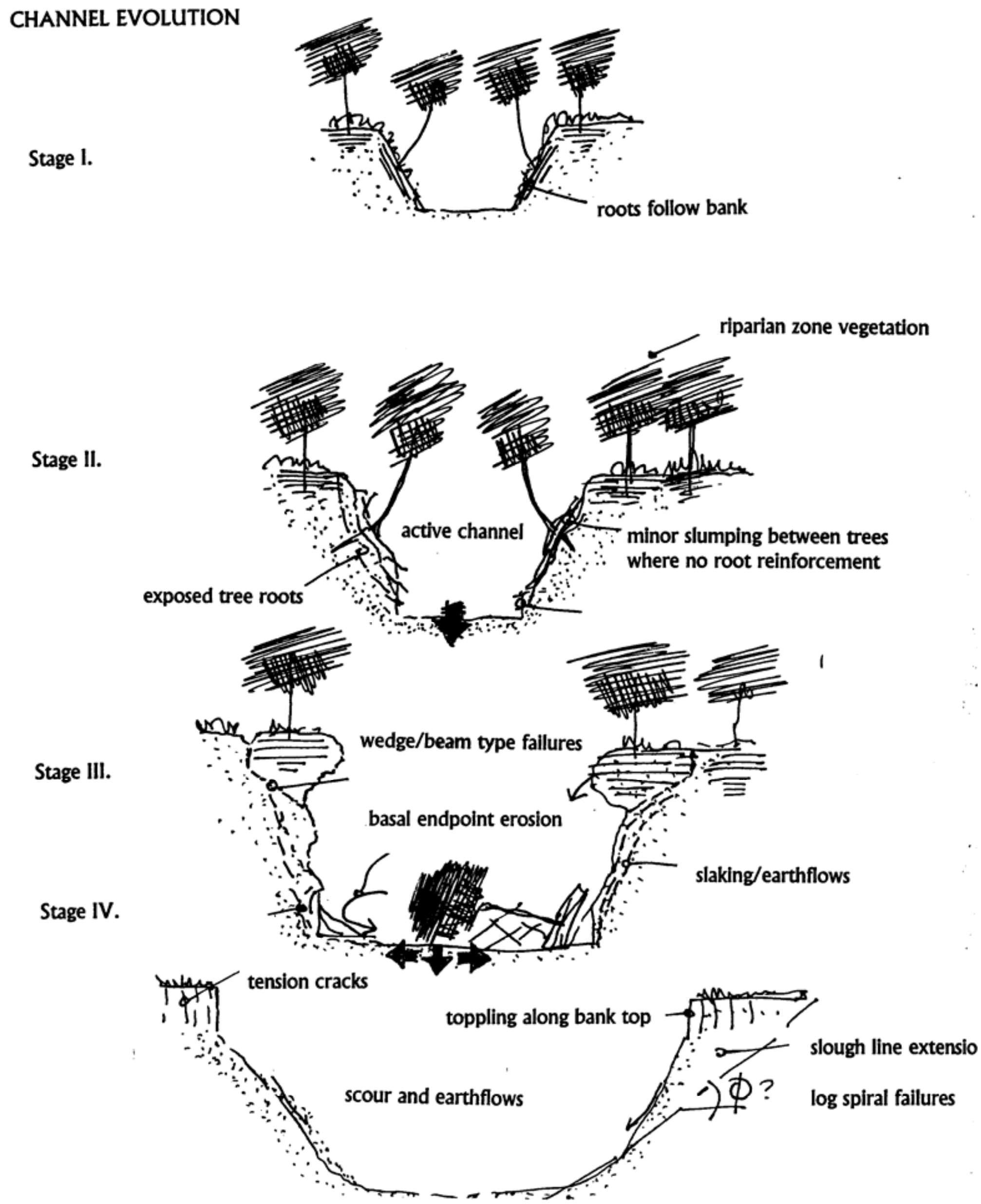

Figure 7. Channel Evolution Model

Figure 8. Degrading Channel CEM II-III (Location 19); Sandy loam soils.

Figure 9. Moderate Erosion; CEM II, fine sandy loam; (Location 13)

Figure 10. Stable channel; slight erosion; CEM I (Location 21).

Figure 11. Severe erosion; CEM II-III; silty clay (location 49). Note the knickzone at the bottom of the channel and slope failures on the channel sides.

Survey Form Stream Assessment

Date: / /2006

GPS ____________________

Location: ______________________

____

Channel Slope USGS 7.5 ________

Drainage Area Acres ________

Photos ____________________

1 Channel, Gully, Other

If Gully Note: headcut height?___

2 Riparian Vegetation: Note on bank

3 Texture: gravel, sand, silt, clay silty clay, loam

4 Reach Length Visible_________ft.

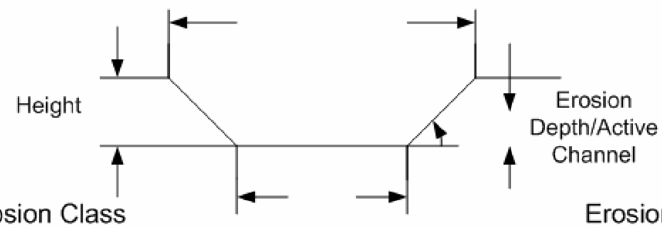

Erosion Class

5 Slight_______
Moderate____
Severe______

Erosion Class

Slight_______
Moderate____
Severe______

6 Bed Material Size (est.)

____

7 Bank Processes

Slumps__
Wedge__
Infinite Slope__

Bank Processes

Slumps__
Wedge__
Infinite Slope__

8 CEM Model Phase
I Stable
II Degrading
III Degrading and Widening
IV Aggrading

PMA

Figure 12. Channel Survey Form

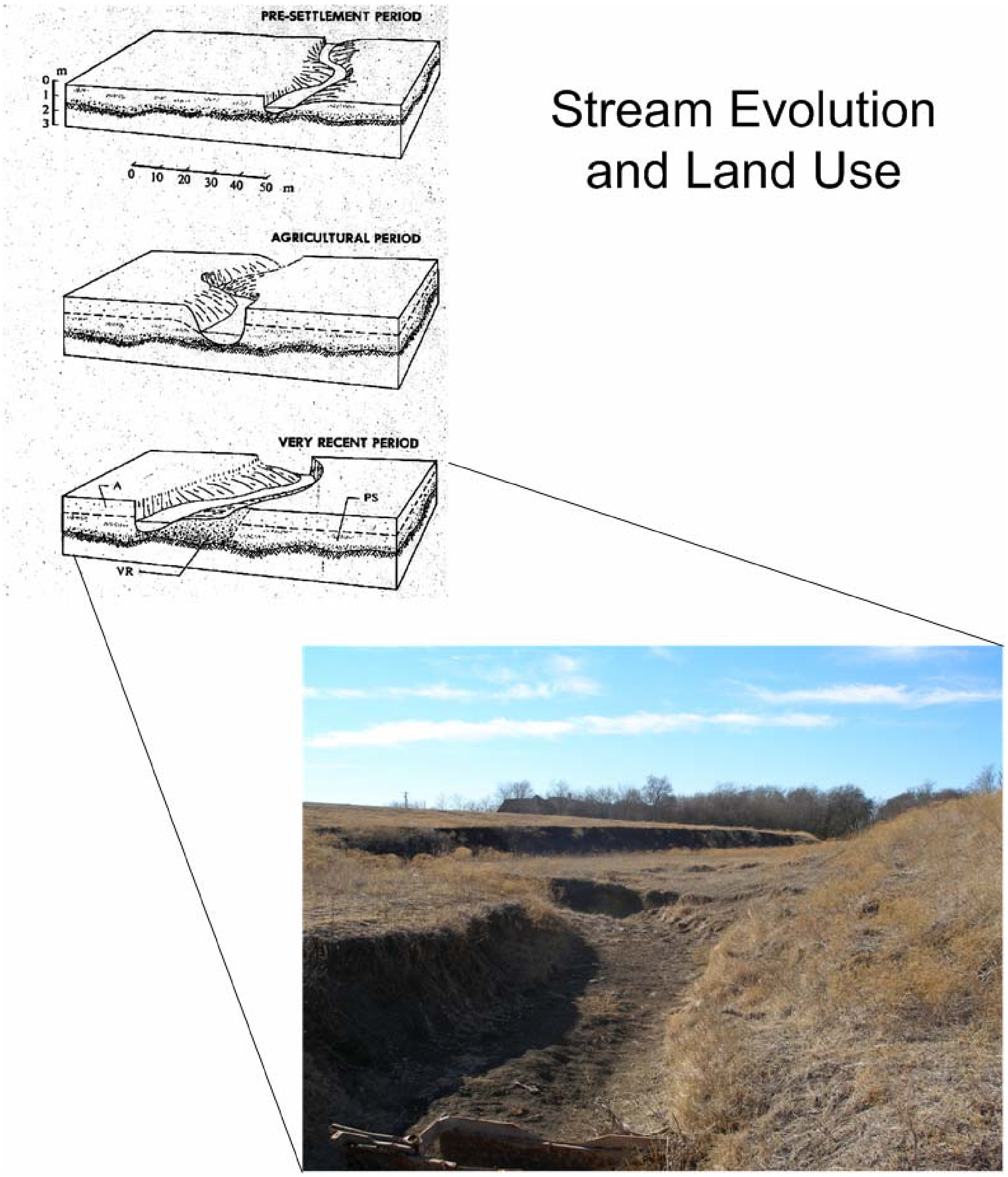

Figure 13. General Change in Streams with Agriculture in United States with example from Cedar Creek. (CEM IV)

Based on the field evaluation forms and limited air photographic analysis, channel segments were classified by degree of erosion.

Rates of erosion were then used with the channel lengths from the model to assess overall erosion using the following equation. It is assumed, for purposes of this analysis that the channel lengths are adjusted for upstream reservoirs.

Tons/yr. = Length x Eroding Height x Erosion Rate x Density (2)

Soil Textural Class	Dry Density For Design (tons/cubic foot)
Organic matter	0.011
Gravel	0.05
Sand	0.055
Silt	0.0425
Clay	0.035

Table 9. Design Densities Soil (MDEQ, 1999).

This calculation, when summed over the channel lengths given in the SWAT model channel length file, yielded 168,182 tons. Average erosion heights of 3 feet were used in this method based on field assessment of erosion (Appendix). Densities are shown in Table 9.

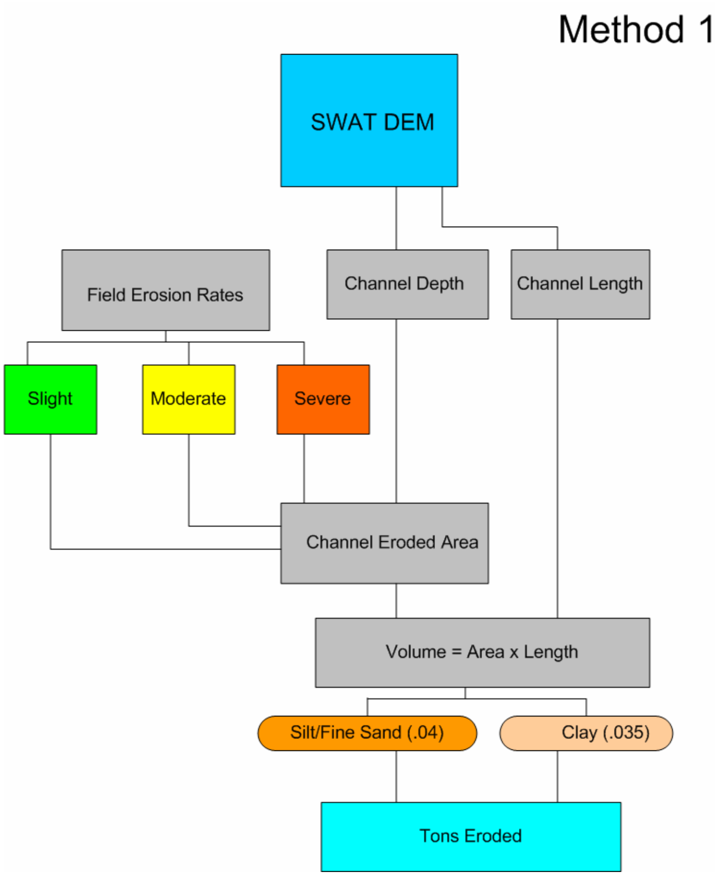

Integration Method

The next method assumed that erosion was more varied along the length of the channel based on drainage basin size and thus a relationship between channel length and drainage basin area was calculated. Channel erosion loss was integrated over the watershed by erosion categories computed from the field surveys for sub-watersheds. This method was based on work by Gregory (1977) for assessing the volume of bankfull channels within drainage basins. Results of this method gave a value of 151,359 tons for the watershed. The result implies that the basic approach of Method 1 gives about the same results as integrating erosion over the whole channel length.

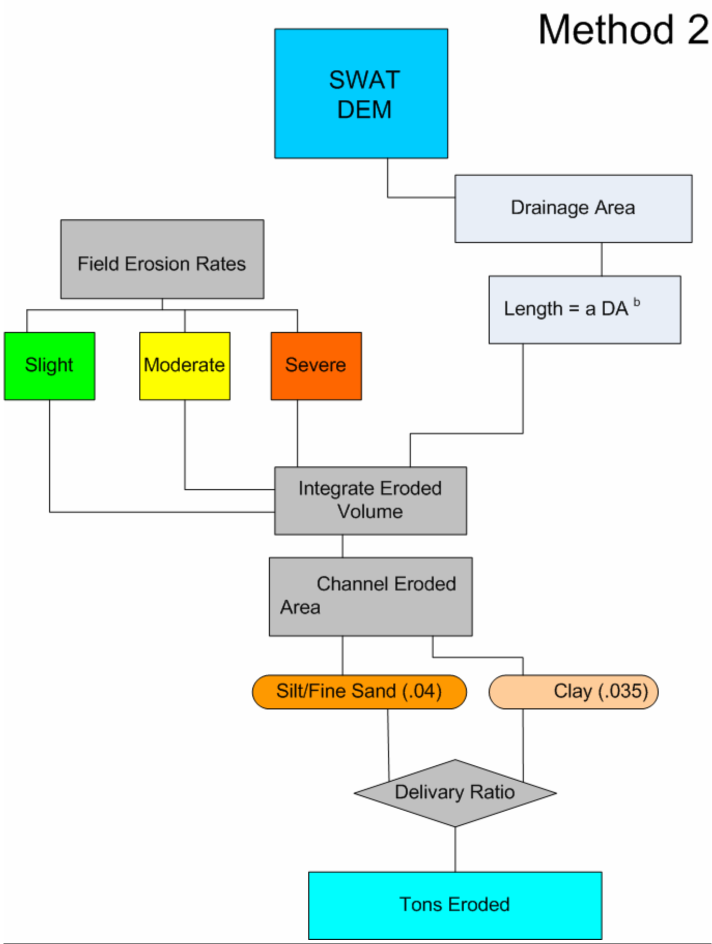

SEDNET Method

An Australian method was utililized based on the stream power approach in which bank erosion is assessed as:

$$BE = .0001\, pg\, Q\, S\, (1\text{-}PR) \qquad (3)$$

Where: *pg* = the density of water and acceleration of gravity
Q = discharge in cms for the 1.58 year flood (USGS 2yr regression)
S = slope of the water surface (taken as the channel bottom slope)
PR = the percent channel vegetation (taken as zero or bare)
BE= annual bank erosion rate in m/year

To calculate the total loss, equation (2) is used substituting the channel erosion rate calculated with equation (3) after Wilkinson, et. al., 2004. The same reach channel lengths are used from the SWAT model as in Method 1.

In the Sednet erosion method, the coefficient is calibrated to yield the average annual bank erosion rate.
The results indicated with bare channels, the rate was 197,684 tons/yr. Average bank vegetation of from 15 to 30 percent would make this method equivalent to the average rate. For purposes of this study and to keep the values consistent, no vegetation effects were used in the calculation.

The Sednet method also employs a gully erosion factor which is added to the stream erosion rate where:

Gully Erosion **= 0.5 x ((0.5 x Soil Density x Cross Section Area)/120 yrs.) x Length**

The linear extent of gullies are mapped for a watershed and used for the gully length. In the Cedar Creek Watershed, the photographic resolution was not sufficient to adequately ascertain the gully density. However, with the available photographs and limited field work, current gully activity was not a major erosion source in the watershed. Ephemeral gully erosion did appear to be a factor in the past, but in this study was not considered to be part of channel and gully erosion but was considered as part of sheet and rill erosion assessment as computed in SWAT using the MULSE procedure.

Gaged Data Comparison

Finally, total suspended sediment yield from the Cedar Creek Basin are computed in the Table 10., below after work by Simon, et. al. (2004) in order to assess the total suspended sediment load observed at gage sites to those values computed in this report for both reservoir yields and for stream erosion.

Tons/yr.	Minimum	25th%	50th%	75th%	Maximum
Without Upstream Control	9519 (104,711)	266,538 (266,538)	1,875,282 (428,364)	3,931,430 (1,589,706)	8,557,761 (3,588,738)
With Upstream Control	3836 (42,340)	107,415 (107,310)	755,739 (172,645)	1,584,366 (640,575)	3,448,778 (1,446,130)

Table 10. Blackland Prairie and (East Central Texas Plains) Ecoregion Values in Tons/year for Suspended Sediment (After Simon, et. al., 2004). (Assume Basin area = 2608 sq. km; assume control equal to 59.7% according to Greiner (1982)).

The numbers in Table 10. are computed as follows:

Tons = Ecoregion Sediment Yeild x Drainage Area x 365 (4)

Where:
Ecoregion Sediment Yeild = tons/day/sq. km.

Ecoregion yields were derived from Simon, et. al, 2004. The Ecoregions mapped in the watershed are the Texas Blackland Prairies and the East Central Texas Plains (Regions 32, 33). The top number computed in the Table corresponds to the Blackland Prairie yeild, the bottom number in parentheses, is the yeild computed for the East Central Texas Plains. The controlled drainage percent is derived from Griener (1982) as previously defined.

Given two assumptions (1) stream and gully erosion is about 65 percent of total erosion as Greiner states, and (2) the Blackland Prairie is approximately 1/3 of the basin, then the weighted average rate of channel erosion and gully erosion would be about <u>225,922 tons/year.</u>

Literature Review Rates

River bank erosion occurs through a combination of mass failure, fluvial entrainment, and subaerial weathering and weakening and thus is a complex process. Literature review of channel erosion rates is somewhat limited as monitoring bank and bed erosion is time consuming and is typically done on small reaches and thus applicability to other geographic areas with different climates, soils, bed material, and vegetation or discharge regimes is always suspect. Such literature still is important in that it shows the range of erosion actually measured in the field and is shown below, Table 11.

Stream Channel	Method and Material	Results
Laubel et. al. 1999 (113.5 sq. km basin in Denmark)	Erosion pins in clayey till and glaciofluvial deposits	Lower bank **11** mm year or 0.02 cubic meters per meter
Allen and others 2005 (Texas Blackland; Ash Creek)	Erosion pins in clay alluvium; one month	**18** mm average; 0.24 cubic meters per meter channel; approximately 0.11 tons per foot channel;
Phillips and others 2005 (42-46,000 sq. km. in Texas, Trinity River)	Historic air photographs; silt sand to clay	30.2 ha over 52 km or 17.4 tons per foot ; 87.6% of annual sediment load; lateral erosion dominant
Prosser and others 2000 (46 sq. km. basin Australia)	Erosion pins and pin surveys in clay	**13 ± 2** mm year or .037 cubic meters per meter
Hooke 1980; worldwide averages; Martin (2005)		Bank m/yr = 0.0245 $DA^{0.45}$; m/yr = $.0475DA^{.4}$
Wohl 1999 (literature); variable sizes	Surveys in sedimentary rock	2-38 mm (**20**)
Booth and Henshaw (2000) Washington	Sand to clay	Less 20 mm to 1 meter year (**510**)

State; 0.1-20 sq. km.		Wide variation, vegetative influences.
Zaimes, et. al. 2005; Iowa 1-3rd order streams	Assumed loam	Severe erosion pasture 143-95 lbs/ft.; pasture no cattle stream and forest; 4.2 to 2.74 lbs/ft.
Couper and Maddock, 2001: cohesive channel; 389 sq. km.	Erosion pins	13-181mm/year

Additional Rates: From Prosser, Hughes, and Rutherfurd, (2000).

Reference	Catchment area (km^2)	Bank height (m)	Bank material	Erosion rate ($mm\ a^{-1}$)
Ripple Creek canal	46	1·5	clay	16
Headwater streams				
Wolman (1959)	10	≈1·0	sand, silt	450–600
Hill (1973)	3·4	2·5–5·5	clay till	30–54
Knighton (1973)	≈15	≈0·6–1·6	glacial till	100–200
Gardiner (1983)	≈20	1–1·5	sand, silt	76–140
Stott (1997)	7·7	≈0·8	peat, glacial till	59
Stott (1997)	6·85	≈0·6	peat, glacial till	47
Lawler *et al.* (1997)	4 km*	–	peat, sand lenses	10–60
Lawler *et al.* (1999)	≈3 km*	1·3	peat, silt clay	71
Lawler *et al.* (1999)	≈9 km*	1	loamy sand	200
Lawler *et al.* (1999)	≈15 km*	3	loamy sand	317
Gully banks				
Crouch and Blong (1989)	2·9	2–7	clay, sand, gravel	5–75
Crouch (1990)	1·2	–	colluvial fill, weathered bedrock	4–53
Crouch and Blong (1989)	–	≈5	sandy clay, weathered bedrock	20
Reid (1989)	–	–	silt, clay	31
Soufi (1997)†	0·1	2	clay, weathered bedrock	11·4
Leopold *et al.* (1966)	9·7	1·5	silty sand	5·7

Table 11. Summary of some literature derived channel erosion rates.

Summary of Channel Erosion Calculations

Method	Modeled Channel Erosion (tons/year)
Model Uncalibrated	**471,052** (Spatial Sciences Lab)
Griener Method (1982)	129,357 (adjusted for upstream reservoirs)
Wilkinson Method	168,182 (SWAT channel lengths)
Integration Method	151,359 (Drainage Area/Length)
SEDNET Method	197,684 (bare channel condition)
Gaged Data Method	225,922 (Assume Blackland 1/3 basin)
Mean (All Methods)	**165,504**

Table 12. Channel Erosion Summary for Cedar Creek Basin.

The mean value is advocated as the design number in this preliminary evaluation of stream channel erosion, Table 12. This is approximately 3 times less than the current SWAT modeled erosion on an annual basis. However, it should be noted that if channels begin to down cut due to land use changes, that the rate computed by the SWAT model would be an appropriate measure of channel erosion.

Summary Points for Channel Erosion

- Simple erosion by weathering on channels in the clay terrain should approach **17 mm (0.6 inches) per year or per flood** minimum. This is for surficial erosion due to weathering and entrainment and does not include bank failure. This would approach a loss rate of 11 pounds per foot of channel. The calculated **average rate for bank erosion in this study was about 134 pounds per foot of channel (.067 tons/ft.)**
- Channel erosion in this study was considered as occurring on one bank in streams in CEM Type I; **If the channel begins to downcut, as in the CEM model, then the erosion rates will accelerate rapidly owing to the fact that both banks and the channel bottom is eroding resulting in over 3 times the reported rates** indicated here. These results have been shown by work by Simon et. al. 2004. This would result in erosion rates on the order of 465,512 tons/year or within 5 Percent of the SWAT modeled results.

- Channel erosion was more severe in clay terrain and in urbanizing areas. Clay is assumed to be transported through the system on an annual basis. Sand transport is slower or lagged. While no calculations were done, it is assumed such movement may be on a decadal scale in terms of downstream transport to the reservoir. In addition, sand deposition will tend to be in reservoir backwater areas as delta deposits; no accumulations of sand were seen in the cores.

Section III: Historic Air Photographic Analysis

Introduction

The Texas Natural Resources Information System (TNRIS) maintains a library of historical aerial photographs that are useful for detecting temporal changes in landscape erosion and management. Historical aerial photographs were taken on a sub-decade basis since the early 1940's in the study area, providing an excellent opportunity to assess changing channel and gully erosion and make inferences on factors that control these processes. We test the relationship between channel and gully erosion against prevailing land cover, climate, and different physiographic zones within the study area. Our goal in this analysis is to assess the relative influence of changing land use and climate, and the physiographic setting on channel and gully erosion.

The study area is divided into three physiographic zones or "land resource areas" (*sensu* Kier et al., 1977) for the basis of our analysis, Figure 4. The B-7 physiographic zone is in the southern portion of the study area and is characterized by sandy and coal-rich bedrock and clay loam soils with low to moderate slope stability and moderate to high plasticity. The B-8/C-5 zone in the center of the study area is an area of sandy bedrock and sandy loam to clay sand soils with moderate to high slope stability and low to moderate plasticity. The C-1 zone to the north of the study area consists of shale bedrock and clay soils with low slope stability and high plasticity.

Methods

Ten locations representative of the three general physiographic zones (B-7, B-8/C-5, and C-1; *sensu* Kier et al., 1977) were selected for the historical aerial photograph analysis (Fig. 14). All available historical aerial photographs for these sites were ordered from TNRIS and were provided as 8.5"X11" photos at different scales centered on the study locations. Most locations had photo records by decades from the early 1940's to the 2004. The percentage of crops, fallow/range, forests, and urban areas was estimated at each locality since the early 1940's. Channel erosion, incised gully expression, and ephemeral gully expression was qualitatively assessed with a relative index from 1 to 5, where 1 = none; 2 = slight; 3 = moderate; 4 = severe; 5 = very severe or worst. No more definitive evaluation could be done owing to the quality of the historic air photographs and the scale of the features being assessed. Since this study focuses on long term, decade scale landscape adjustments, temporal trends in climate are compared to the National Oceanic and Atmospheric Administration (NOAA, website) records of ENSO events. El Niño events typically result in more precipitation, while La Niña usually results in droughts in the American southwest (Glantz, 2001). Thus, documented El Niño years are assigned a value of +1, La Niña events -1, and normal years 0. A ten year running average of ENSO conditions is compared to temporal changes in channel and gully erosion indices in this study to assess any relationships between long term trends in climate and the decade scale resolution of the aerial photograph analysis.

Results

Agricultural operations dominate land use within the study area, accounting for >50% of the area since the early 1940's. There seems to be a weak correlation between the amount of fallow land and ephemeral gully expression in the clay-rich C-1 zone (Fig. 15C). There is a near inverse relationship between channel and gully erosion trends between the sandy zones (B-7 and B-8/C-5) and the clay dominated zone (C-1) in Figure 15. Figure 16 illustrates a very weak correlation between channel erosion and time for the whole study area, which is similar to the trends expected for both incised and ephemeral gully erosion.

Figure 17 shows temporal trends of channel and gully erosion by physiographic zone superimposed on the ten year running average ENSO trends. All channel and gully erosion regression trends are based on fourth-order polynomials (Fig. 14). Channel and gully erosion in the sandy physiographic zones (B-7 and B-8/C-5) result in a pseudo-sine wave with very good predicted versus measured correlation and closely reflect ENSO trends (Figs. 17A,B). On the other hand, the clay terrain zone (C-1) has weak statistical predictability coupled with poor covariance with ENSO trends.

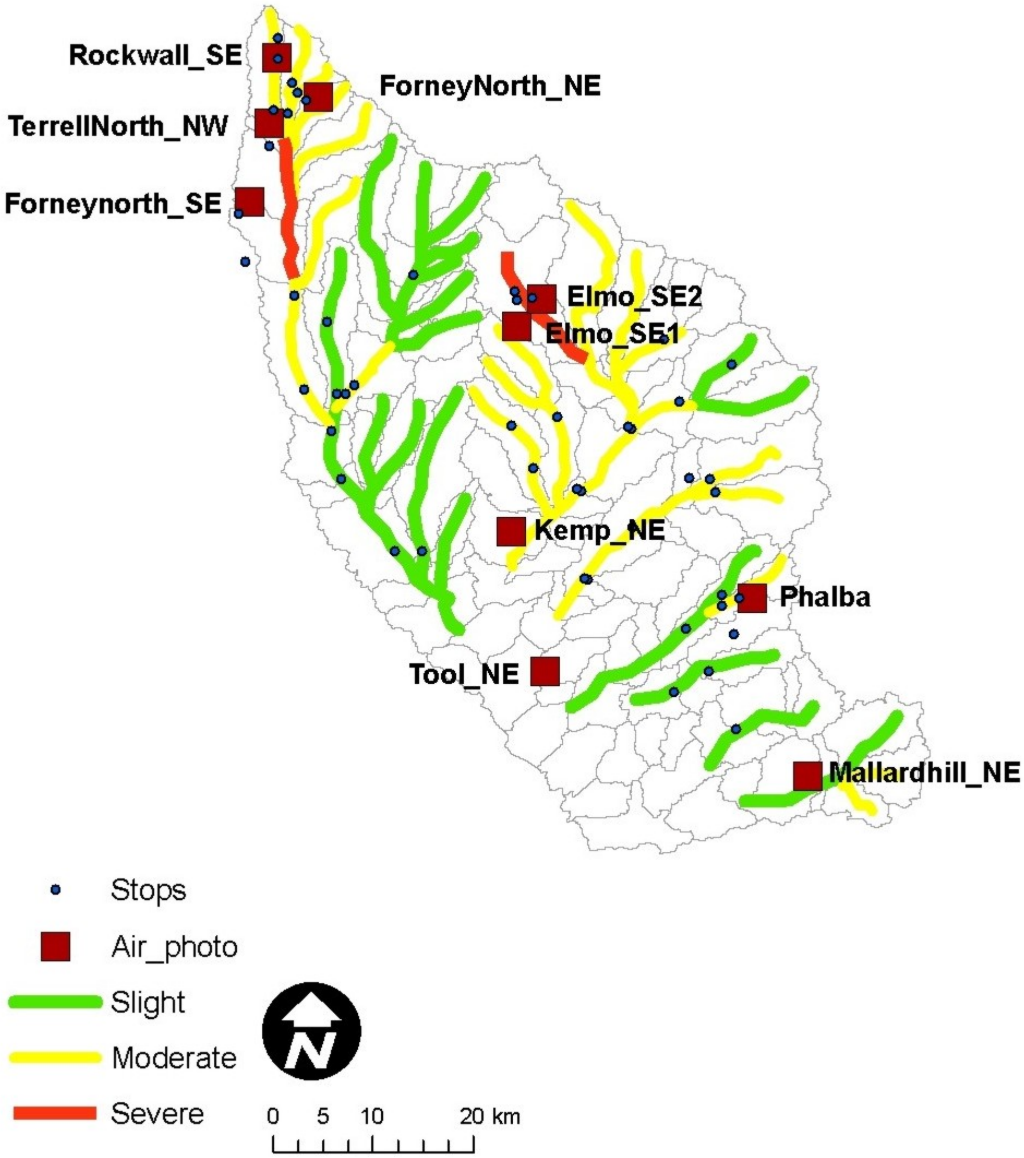

Figure 14. Air photograph locations, field assessment stops, and current channel erosion.

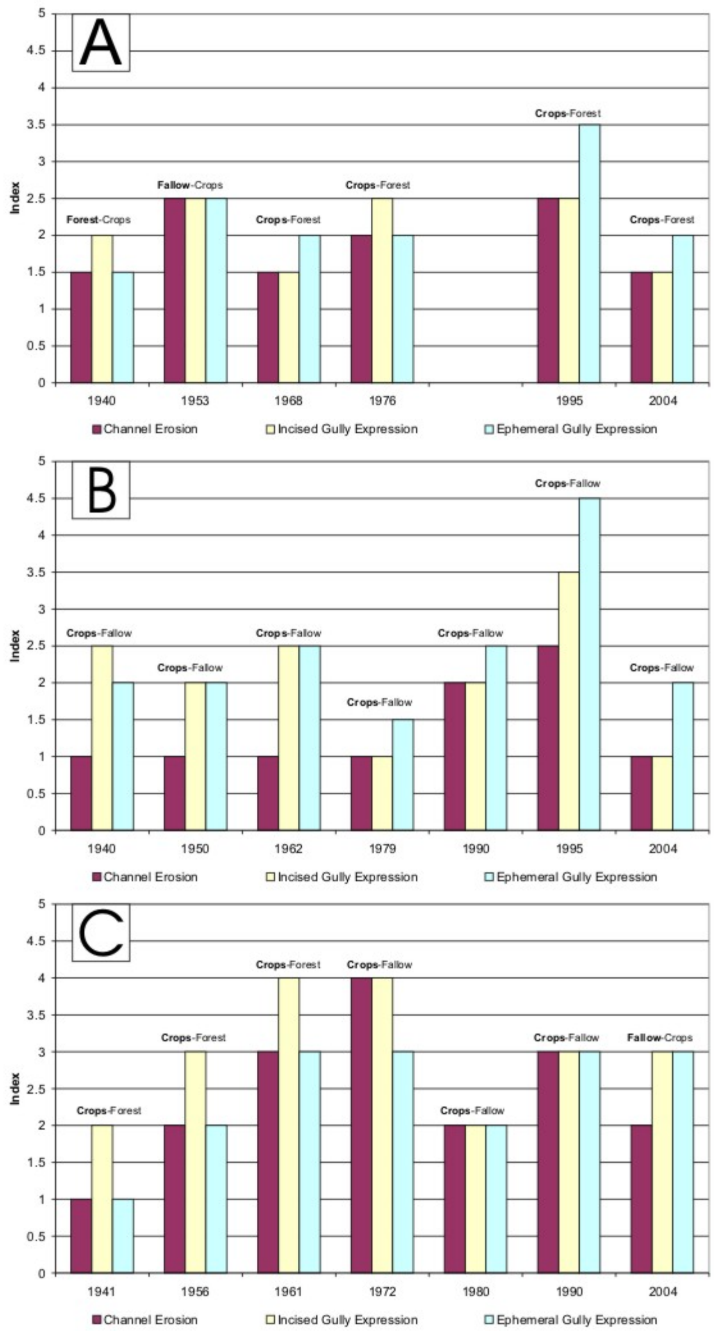

Figure 15. Temporal variability of channel and gully erosion indices (1=none; 2=slight; 3=moderate; 4=severe; 5=very severe) and land use at representative locations for the three general physiographic zones within the study area. The dominate land use is portrayed in bold, while the second most common land use is standard text above the erosion bars. A.) Mallard Hill quadrangle in the B-7 zone. B.)

The Elmo Southeast quadrangle in the B-8/C-5 zone. C.) The Terrell North quadrangle in the C-1 zone. Notice the inverse trends in the sandy zones (B-7 and B-8/C-5) versus the clay dominated C-1.

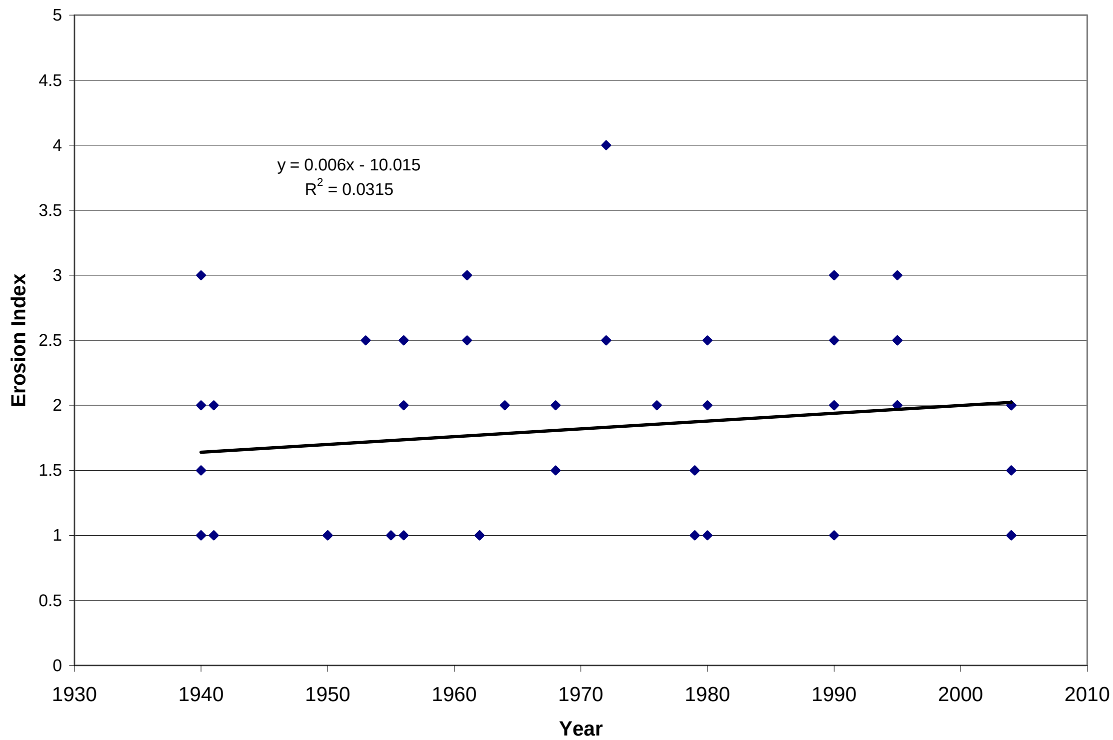

Figure 16. The relationship between time and channel erosion across the whole study area is very weak. The weak correlation suggests that there are physiographic distinctions since climate is considered to be the same over the study area.

Discussion

Land use change, as detected on the air photographs has not been of significant magnitude to influence channel and gully erosion fluctuations observed in Figure 15. There is no observable connection between the changing proportions of land cover and most erosion indices seen on the photographs. However, the correlation between fallow land cover and ephemeral gully expression in the clayey zone (C-1) suggests that ephemeral gullies may develop more rapidly in clayey soils without cover (Fig. 2C).

The nearly opposite temporal trends in channel and gully erosion indices between the sandy (B-7 and B-8/C-5) and clayey (C-1) zones in Figure 12 suggests that substrate grain size is a key element in landscape response to some presumably extrinsic factors (i.e. climate. Figure 16 supports this interpretation by plotting channel erosion indices against time with a very weak statistical covariance. This weak correlation suggests that there are physiographic distinctions in channel erosion since extrinsic factors like climate are considered to be constant across the small study area.

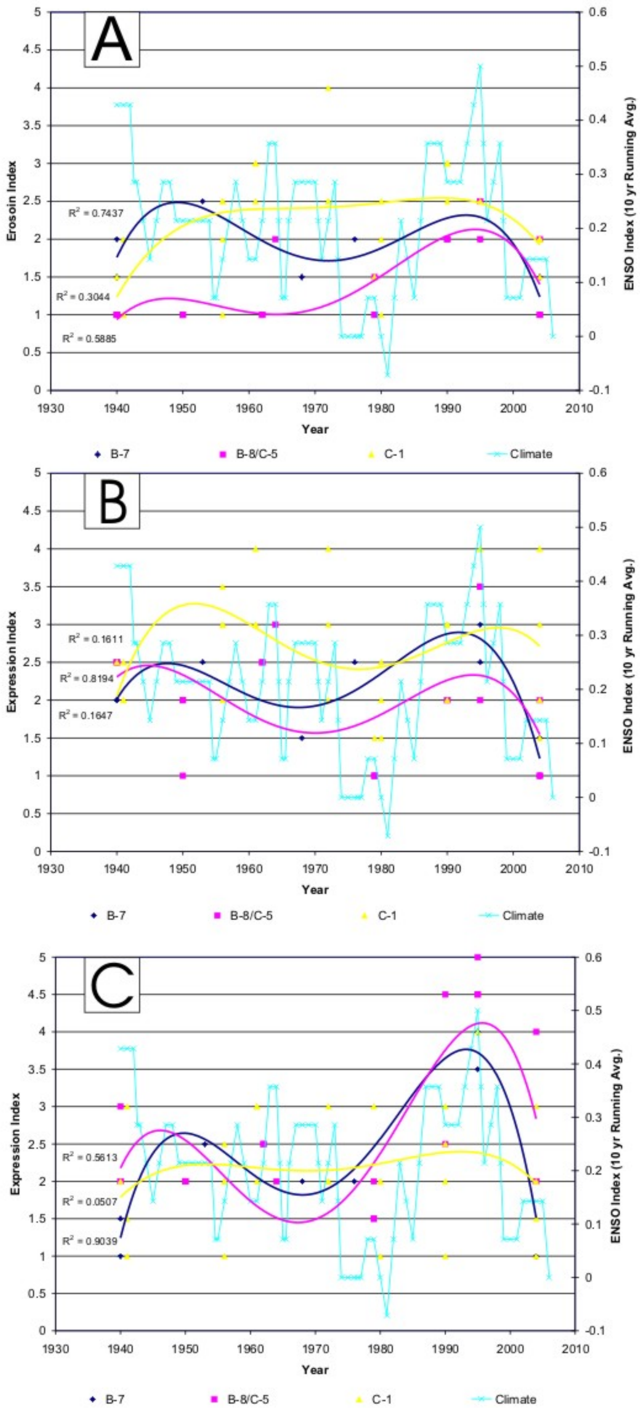

Figure 17. Temporal trends of channel and gully erosion by physiographic zone superimposed on the ten year running average ENSO trends. All channel and gully erosion regression trends are based on fourth-order polynomials. A.) Channel erosion; B.) Incised gully erosion; C.) Ephemeral gully erosion.

Channel and gully erosion in the sandy zones (B-7 and B-8/C-5) result in a double, pseudo-sine wave with very good predicted versus measured correlation and closely correspond to ENSO trends. This suggests that each physiographic zone has a unique landscape erosion response that is easily detectable on a decade scale and that erosion in sandy terrains is apparently controlled by climate. On the other hand, poor statistical predictability coupled with poor covariance with ENSO trends suggests that the visible changes in clay terrains are independent of longer term climatic cycles. In fluvial systems, substrate particle size and climate have been shown to influence long term geologic scale (100's to 1000's years) changes in intra-basin sedimentation and erosion (Miall, 1992). However, we demonstrate that these factors may influence channel and gully erosion on a very rapid time scale (within 10 years).

The connection of profound changes in fluvial erosion to relatively short-term (in the geological sense) ENSO trends has profound implications for the future of sediment yield from the study area. ENSO conditions will almost certainly change in response to global climate warming, with predictions of 1.5 to 6.0 ºC rise in mean temperature in the next 100 years (Tudhope, 2003). Variability in ENSO expression has resulted in multiyear to multi-century persistence in either strong El Niño or La Niña conditions that would be devastating to current projections of sediment yield. For example, persistent La Niña conditions resulted in prolonged drought conditions across the western U.S. between 1855 and 1863 (Cole et al., 2002) for which there is no analogue in modern weather observations. On the other hand, climatic shifts which favor El Niño conditions usually result in more available moisture in the Southwest, which may increase fluvial erosion, sedimentation, and nutrient loading especially if preceded by a strong La Niña. Fraticelli (2004) documents this phenomenon in terms of fluvial erosion and deltaic sedimentation on the Brazos River of Texas. Similarly, Prochnow (2001) finds evidence for pronounced flooding and sedimentation during El Niño episodes during the early Holocene (~8,000 years ago) and Historic times on the Brazos River. Given this evidence, planners should expect more variability in fluvial erosion and subsequent sediment yield than observed in aerial photograph records since the early 1940s.

Summary from Air Photographic Analysis

- Land use changes have not been dramatic within the basin and have not significantly influenced channel or gully erosion as seen on historical photographs. More recent urbanization in Upper Brushy Creek needs to be monitored. Newer high quality air photographs will permit more accurate evaluation of channel changes in the future
- Physiographic setting related substrate particle size is correlated to the fluvial response to climate in the watershed
- ENSO trends and climate appear to be a factor in controlling erosion in the sandier subwatersheds
- Fluvial erosion in the clay terrain appears to be less affected by the longer term climate cycles and seems to be fairly consistent on an annual cycle. This is attributed to clay weathering cycles with seasonally wetting and drying and thus providing a constant supply of fine, easily transportable material for smaller flood events.

Section IV: Future Considerations

In the case of all surveys and modeling efforts, better results can be obtained with better data inputs. With regard to the Cedar Creek Reservoir, the following suggestions are made in an effort to better calibrate the modeling efforts and make assessment of future management and land use scenarios more precise.

1. **Channel Erosion Assessment**: It is recommended that erosion pins and scour chains or monitoring sites be installed on major stream channels. A statistical sampling of stream erosion based on field data by soil/geology could give a far better assessment of erosion loss rates. Such methods are being done on large areas in the United States (see Zaimes, et. al, 2006). In addition, within these areas, it is recommended that submerged jet test be done to assess Tc and K values by alluvial soil type so that the results can be directly put into the SWAT model and calibrated. It is estimated that only about 6 jet tests would be needed in order to quantify these initial values. The erosion pins and scour gages can be quickly installed, left for a period

of a year or more, and then resurveyed. Methods are well established and sampling can be done easily and results can be used to calibrate models. About 100 sites could be installed by physiographic area and drainage area (stream order) and land use to give some meaningful rates of lateral and vertical erosion. Stream size prohibits meaningful photogrametric work.

2. **Land Use Change**: It appears as if the upper Brushy Creek area is beginning to undergo urbanization. Land use changes will affect stream erosion and without potential detention, this will effect streams stability. NCTCOG guidelines with regard to detention should be investigated. Without detention, channels will degrade following the CEM model. The amount of erosion potential from such degradation is very large, eg. in the order of tons per foot of channel and can have the effect of increasing loads from channel erosion by a factor of 3.
3. **Long Term Basin Erosion/Floodwater Surveys**: Surveys of small floodwater structures in the upper basin can give better estimates of sheet/rill and ephemeral gully erosion for model calibration. This can be done quickly and with high precision. These should be chosen by soils/geologic province, age of structure, and land use changes within the sub-watershed. Using a combination of floodwater structure sedimentation rates in the uplands with cumulative rates from the reservoir will again enhance calibration of the basin sediment model.
4. **Short Term Sediment Transport Monitoring/Turbidity Sensors**: Installation of turbidity sensors on major tributary inputs to the lake with some preliminary calibration could give excellent data for future model calibration and assessment of watershed trends. These systems are now quite reasonable and require, after calibration, minimal field time to download, or can be attached to cellular phones or hard-lined to the office.
5. **Sand versus Clay Terrain:** There are distinct differences in the basin in terms of channel erosion potential which follow the outcropping geologic units. Knowledge of these provinces coupled with land use changes is necessary for proper evaluation of stream erosion response.

References:

Cole, J.E., Overpeck, J.T., Cook, E.R. 2002. Multiyear La Niña events and persistent drought in the contiguous United States: Geophysical Research Letters, 29, 13, 25-1 to 25-4.

Fraticelli, C.M. 2004. The effects of ENSO cyclicity on deltaic progradation; examples from the modern Brazos Delta. Abstracts, Geological Society of America, Vol. 36, 5, pp. 192.

Glantz, M.H. 2001. Currents of Change: El Niño's and La Niña's Impact on Climate and Society. Cambridge University Press.

Kier, R.S., L.E. Garner, L.F. Brown, Jr., 1977. Land Resources of Texas, Special Report. Bureau of Economic Geology, University of Texas at Austin, Austin, Texas. 45 p.

Miall, A.D., 1992. Alluvail Deposits in Walker, R.G. and James, N.P., eds. *Facies Models: Response to Sea Level.* Geological Association of Canada, Gloucester, Ontario, pp. 119-142.

Prochnow, S.J. 2001. Geoarchaeology and slackwater paleoflood modeling at Horn Shelter No. 2 along the Brazos River: Bulletin of the South Texas Geological Society, 42, 1, 15-25.

Roberts, N. 1998. The Holocene: An Environmental History 2nd Ed. Blackwell, Malden, Mass.

Tudhope, S. and Collins, M. 2003. The past and future of El Niño: Nature, 424, 261-262.

Laubel, A., Svendsen, L.M., Kronvang, B., Larsen, S.E., 1999. Bank erosion in a Danish lowland stream system. Hydrobiologia, 410: 279-285.

Phillips, J.D., Slattery, M.C. and Musselman, Z.A., 2005. Channel adjustments of the lower Trinity river, Texas, downstream of Livingston dam. Earth Surface Processes and Landforms. 30: 1419-1439

Wolman, M.G., 1959. Factors influencing erosion of a cohesive riverbank. Amer. Journal of Science: 257:204-216.

Prosser, I.P., Hughes, A.O., and I.D. Rutherfurd. Bank erosion of an incised upland channel by subaerial processes:Tasmania, Australia. Earth Surface Processes and Landforms, 25:1085-1101.

Hooke, J.M., 1980. Magnitude and distribution of rates of river bank erosion. Earth Surface Processes, 5:143-157.

Windhorn, R.H., 2001. RAP-M: Rapid Assessment Point Method. NRCS, Champaign, Ill. Misc. pages.

Wohl, E.E., 1999. Incised bedrock channels (In) Incised River Channels: processes, forms, engineering, and management (eds.) S. Darby and A. Simon, Wiley, pp. 187-218.

Booth, D. and Henshaw, P.C. (2000) Rates of channel erosion in small urban streams. (In) M. Wigmasta, ed. Stream Channels in Disturbed Environments: AGU Monograph Series.

Zaimes, G.,N., Schultz, R.C., Isenhart, T.M., Mickelson, S.K., Kovar, J.L., Russell, J.R., Powers, W.P., 2005. Stream Bank Erosion Under Different Riparian Land-Use Practices in Northeastern Iowa. AFTA Conference Proceedings. pp. 1-10.

Couper, P. and I. P. Maddock, 2001. Subaerial river bank erosion processes and their interaction with other bank erosion mechanisms on the River Arrow, Warwickshire, UK., Earth Surface Processes and Landforms, 26, pp 631-646.

Kier, R.S., Garner, L.E., Brown, L.F., 1977. Land Resources of Texas. Bureau of Economic Geology, University of Texas, Austin, Texas. Misc. pages.

Wilkinson, S., Henderson, Anne, Chen, Yun, 2004. SEDNET, Version 1.0. User Guide. Client Report for the Cooperative Research Centre for Catchment Hydrology; CSIRO Land and Water Canaberra, Australia.

Allen, P.M., Arnold, J.G., and Skipwith, W., 2002. Erodibility of urban and alluvial channels, North Texas. AWRA, Vol 38, No.5, pp. 1477-1492.

Allen, P.M., Arnold, J.G., and Byars, B.W., 1994. Downstream channel geometry for use in planning level models. AWRA, Vol. 30, NO.4, pp. 663-671.

Zaimes, G.N., Schultz, R.C., and Isenhart, T.M., 2006. Riparian Land Uses and Precipitation Influences on Stream Bank Erosion in Central Iowa. JAWRA, vol 42(1), pp. 83-97.

Simon, A., Dikerson, W, Heins, A., 2004. Suspended sediment transport rates at the 1.5 year recurrence interval for ecoreigons of the United States: transport conditions at the bankfull and effective discharge? Geomorphology, vol 58, pp. 243-262.

MDEQ, 1999. Surface water Quality Division Pollutants Controlled Calculation and Documentation for Section 319 Watersheds Training Manual.

Simon, A. 1989a. The discharge of sediment in channelized alluvial stream. Water Resources Bulletin 25 (6), 1177-1188.

Simon, A. 1994. Gradation processes and channel evolution in modified West Tennessee streams: process, response, form. U.S. Geological Survey Professional Paper 1470. USGS Wash. D.C. 84p.

Schumm, S.A., Harvey, M.D., Watson, C.A., 1984. Incised Channels: Morphology, Dynamics and Control. Water resources Publications, Littleton, CO. 200p.